https://doi.org/10.5194/egusphere-2026-1627
Preprint. Discussion started: 9 April 2026

Mediterranean Sea surface currents obtained with a variational inverse method, insight on the central Ionian Sea

Abel Dechenne[1], Aida Alvera-Azcarate[1], Jean-Marie Beckers[1], and Alexander Barth[1]
[1]University of Liege, Liege Belgium
Correspondence: Abel Dechenne (adechenne@uliege.be)

Abstract. The surface currents of the Mediterranean Sea are interpolated with a variational inverse method for nine years (2013-2021). The general method is called DIVAnd and was adapted here specifically for surface currents as it considers the presence of the coastline and a divergence constraint. For the interpolation, three data sources are used; satellite altimetry, drifters and high-frequency radars. A subset of drifters (10%) is used to calibrate the parametrization and to validate the results. Moreover, the results are compared with the geostrophic product computed per DUACS (Copernicus Marine Service, 2023) and was shown to be less accurate than the DIVAnd results. Using the new results, summer and winter seasons were averaged and compared to capture the most consistent patterns. At the basin scale, we concluded that the winter to summer variation is a shift between a coastal, large and well-defined currents to a variable and gyral circulation. In addition, we decomposed the Ionian Sea into orthogonal functions to investigate the appearance of what we called the Twin Gyres (TGs). These gyres, that settle around 36°N-17°E on the second part of the year, first appeared in the central Ionian Sea in 2020. The TGs were found to modify consequently the temperature profile of the central Ionian Sea. The mode decompositions showed it to be associated with the Atlantic Ionian Stream velocity and being associated with a temperature front, situated between the Adriatic waters and the southern Ionian waters.

1 Introduction

Since the emergence of satellite altimeters during the second half of the twentieth century (Le Traon et al., 2025) , the study of surface dynamics has been consequently expanded, refining our understanding of the global circulation patterns.

Recently, the number of sampling tools to observe the sea has increased significantly (Wilkinson et al., 2024) and their access was facilitated with online platforms such as Copernicus or EMODnet, providing validated and documented datasets. Among the variety of these datasets, three of them are particularly valuable to observe the surface currents; satellite altimetry (sea level), drifters, and High Frequency radars (HF Radar). Although these tools share the common capability of measuring surface currents, each operates with distinct temporal sampling frequencies and spatial coverage ranges.

Satellites have monitored the global ocean for several decades and provide an overall estimate of currents on a large scale through altimetry. Indeed, sea-level anomalies are used to estimate surface velocities under the geostrophic assumption, which is generally valid at large spatial scales characterized by low Rossby and Ekman numbers (Beckers and Cushman-Roisin, 2011).

https://doi.org/10.5194/egusphere-2026-1627
Preprint. Discussion started: 9 April 2026

However, because this assumption comes less and less valid at small scales, mesoscale and sub-mesoscale events cannot be resolved, particularly under 100km of resolution. Despite these limitations, satellite altimetry represents the major source of data to provide surface current estimates and is widely used in surface current studies, (e.g. Cotroneo et al. (2016); Poulain et al. (2013); Soto-Navarro et al. (2010); Martínez et al. (2024)).

A major part of surface currents studies rely on in-situ observations obtained from drifters and/or gliders. These platforms drift with the near-surface flow, providing the most direct measurement of surface and near-surface dynamics. Therefore, they are frequently used for the validation and to increase the robustness of surface current analysis (e.g. Capodici et al. (2019); Corgnati et al. (2024); Menna et al. (2019a)). However, their spatial distribution is sparse, especially in high latitude regions (Lumpkin and Johnson, 2013). We note also that their trajectory is influenced by the wind speed, the wave height and the various internal oscillation within the upper layer (Delpeche-Ellmann et al., 2021).

High-Frequency Radars, introduced in the late twentieth century, have become an important tool for coastal observations, as they measure currents via a Doppler shift. These antennas monitor surface dynamics in a range of 85 km from the coast with hourly temporal frequency and fine spatial accuracy, often going under 4 km (Barth et al., 2021). Within the Mediterranean Sea, HF Radars are used for small scale currents pattern analysis such as the study of the Strait of Gibraltar (Soto-Navarro et al., 2016), Balearic Island dynamics (Troupin et al., 2015) or Sicily channel (Capodici et al., 2019). They are also used in many other regions in the world to analyze meteorological and climatic phenomena e.g. Domps et al. (2022); Frissell et al. (2016); Liu et al. (2021).

The objective of this paper is to perform a large scale interpolation of the surface circulation of the Mediterranean Sea using Satellites, Drifters and HFRadars within the same framework. The combination of these different datasets is necessary to obtain a sufficient coverage as the data distribution of drifter and HF radar data is highly heterogeneous. Since the average currents of the Mediterranean Sea are well known (e.g. Pinardi et al. (2015); Iacono et al. (2013); Martínez et al. (2024)), the main objective of the study is to contribute to the knowledge of the seasonal, inter annual and climatic variations at the basin scale. This issue is addressed using a variational inverse method documented in (Barth et al., 2021). To this end, nine years of observations corresponding to the period 2013-2021 will be used to reconstruct the monthly surface current of the whole basin of the Mediterranean Sea.

2 Mediterranean Sea Surface Currents review

The Mediterranean Sea is viewed by the scientific community as a “miniature ocean” due to its short water residence (corresponding to a tenth of the global ocean time) and its thermohaline circulation comparable to the global ocean (Adloff et al., 2015). Therefore, defined as a hot-spot to observe the major impacts of global warming, its response to climate change is expected to be faster than the global ocean. Thus, the impact of climate change can be seen on a lifetime period and then, make its study of a primary importance (Malanotte-Rizzoli et al., 2014).

https://doi.org/10.5194/egusphere-2026-1627
Preprint. Discussion started: 9 April 2026

Western Mediterranean Sea	
Atlantic Waters	AW
Western Alboran Gyre	WAlbG
Eastern Alboran Gyre	EAlbG
Algerian Current	AC
Western Algerian Gyre	WAlgG
Eastern Algerian Gyre	EAlgG
Sicily Channel	SC
Tyrrhenian Current	TC
Eastern Corsica Current	ECC
Western Corsica Current	WCC
Northern Current	NC
Gulf of Lion Gyre	GLG
North Balearic Current	NBC
Eastern Mediterranean Sea	
Atlantic Ionian Stream	AIS
Atlantic Tunisian Current	ATC
Northern Ionian Gyre	NIG
Mid Ionian Jet	MIJ
Lybio Egyptian Current	LEC
Cyprus Current	CC
Asia Minor Current	AMC
Mersah-Matruh Gyre	MMG
Rhode Gyre	RG
Ierapetra Gyre	IG
Pelops Gyre	PG

Table 1. Lists of acronyms.

The Mediterranean Sea has a counterclockwise circulation, occurring in two separated sub-basins (western and eastern basins). These sub-basins are partially isolated one from another by the Sicily Channel, acting as a physical barrier, due to the reduced depth of its continental shelf. Along with that, its complex bathymetry makes the coastlines and the continental slopes an important factor to constraint the current. Most of the studies measure currents below 1 m/s with strong currents at the border of the domain, while the middle ocean is populated by cyclonic and anticyclonic gyres and eddies. The following section will describe the existing knowledge of the Mediterranean Sea surface current and is summarized in Figure 1. It starts with the penetration of Atlantic Water (AW) at the Strait of Gibraltar for the western basin and will describe the circulation of

https://doi.org/10.5194/egusphere-2026-1627
Preprint. Discussion started: 9 April 2026

the eastern basin, starting with the description of the circulation of the Sicily Channel (SC).

2.1 Western Mediterranean Sea

Alboran Sea

In the western part of the sea, the Atlantic Waters (AW) enter the Mediterranean Sea through the Strait of Gibraltar with a mean estimated to 0.81 ± 0.06 Sv (Soto-Navarro et al., 2010). The AW inflows the Alboran basin, known to have a complex circulation populated by two or three large permanent gyres (Renault et al., 2012). These patterns exhibit two or three times more energy during summer months compared to winter periods. Their dynamics are complex and are known to vary in response to changes in the transport through the Strait of Gibraltar (Renault et al., 2012). The AW follows the gyres from west to east, ultimately directed towards the Algerian Coast.

Algerian Current

The AW then exits the Alboran Sea and flows along the African continental slope between 0°E and 10°E forming the Algerian Current (AC). It is known to be a strong permanent current, to which is associated two large permanent gyres; Western Algerian Gyre (WAlgG) and Eastern Algeria Gyre (EAlgG) (e.g. Testor et al. (2005); Mallil et al. (2022)). This current is agreed to be highly turbulent, impacted by baroclinic instabilities, forming meanders, and leading to intense eddy formation migrating to the north (Poulain, 2012; Cotroneo et al., 2016; Pessini et al., 2018; Mallil et al., 2022).

Tyrrhenian Sea

Once at the northern part of the Sicily Channel, the AC has two options; a part of the water will be kept in the western part of the sea and will enter in the Tyrrhenian Sea while the remaining AW will cross the Sicily Channel (SC). The current entering the Tyrrhenian Sea will be called the Tyrrhenian Current (TC), which is known to exhibit strong variations with winter-summer seasonality. The late winter and early spring patterns can be described with a consistent strong cyclonic flow along the coast. On the other hand, the summer circulation is associated with the collapse of the coastal current, which is much more variable and associated with the appearance of coastal gyres (Iacono et al., 2013, 2021).

Northern Current and Balearic Islands

Northward, we find the Corsica channel and further, the Liguro-Provencal Basin, where a non-negligible part of the TC will flow. In the Liguro-Provencal Basin, the along slope current is called the Northern Current (NC) and is controlled by thermohaline circulation, the northern shelf edge and the wind (Poulain, 2012; Carret et al., 2023). This latter varies in velocity between summer and winter, being faster in winter, reaching 0.9m/s (Poulain, 2012). The NC will flow alonglsope until the Balearic Island longitude. Offshore the Gulf of Lion, we find a permanent large cyclonic circulation called the Gulf of Lion Gyre (GLG) (Pinardi et al., 2015).

https://doi.org/10.5194/egusphere-2026-1627
Preprint. Discussion started: 9 April 2026

Further, most of the studies report the return of the NC through the North Balearic Current (NBC), flowing eastward in the center part of the western Mediterranean Sea (around 40°N) (Vargas-Yáñez et al., 2025). However, a non-negligible amount of water will cross the Ibiza channel section. Recent literature documented the transport within the Ibiza and Mallorca channels and highlighted a dominance of the southward flow within the Ibiza channel and a northward flow within the Mallorca channel (Vargas-Yáñez et al., 2025, 2023).

2.2 Eastern Mediterranean Sea

Sicily Channel and Ionian Stream

Coming back to the SC, a non-negligible part of the AC forms one (or two depending on the season) jet that crosses the SC and enters the Eastern part of the Mediterranean Sea (Jebri et al., 2016). The seasonal transport through the strait has a maximum value of 1.4Sv in winter and a minimum value of 0.8Sv at the end of summer (Béranger et al., 2004). First, the strongest and the most resilient flow found after the SC is the Atlantic Ionian Stream (AIS), directed by the Sicily continental slope (Jebri et al., 2017; Jouini et al., 2016). Second, the flow can follow the Tunisian coastline via the Atlantic Tunisian Current (ATC). This current has a high seasonal and spatial variability, known to be weaker in summer due to surface easterly winds (Jouini et al., 2016; Martínez et al., 2024). However, the lack of in-situ observations and its low velocity in summer makes its detection complex compared to the AIS (Sammari et al., 1999; Jebri et al., 2016; Jouini et al., 2016).

Ionian basin

Further, the Ionian Sea is characterized by two main currents. First, the Northern Ionian Gyre (NIG) follows the northern boundary of the basin, cyclonically or anti-cyclonically depending on the thermohaline situation of the basin (Menna et al., 2019b; Meli, 2024; Demirov and Pinardi, 2002). This latter is described by a decadal/sub decadal reversion where the last reversion occurred in 2019 going from anticyclonic to cyclonic. The "decadal" term i.e. Menna et al. (2019b) is under debate due to the recent shorter variations (Napolitano et al., 2025; Borzelli et al., 2009; Liu et al., 2022; Meli, 2024). Its complex mechanism is described in Civitarese et al. (2023). Second, the Mid Ionian Jet (MIJ) crosses the basin going southeastward, joining the Cretan Passage. This basin is known for its complex bathymetry and for the local wind stress, inducing instabilities and numerous vortices within the MIJ (Menna et al., 2019b). When the NIG is flowing cyclonically, the MIJ is reported to be an intense (10-20cm/s) south-eastward current while, during the anticyclonic phase of the NIG, the MIJ is less intense and more fragmented, with velocity under 10 cm/s (Menna et al., 2019b).

Cretan Passage and Levantine basin

Further, MIJ waters enter the Levantine Basin by the Cretan Passage, becoming an along slope current, the Lybio-Egyptian Current (LEC). In a big picture, the circulation of the Levantine basin is cyclonic and reaches Egyptian longitudes via the LEC. There (around 30°E), the LEC bifurcates; The first branch reamins an along slope cyclonic circulation, while the other one

https://doi.org/10.5194/egusphere-2026-1627
Preprint. Discussion started: 9 April 2026

flows seaward (northward) toward the south-west Cyprus coast. The seaward flow is called the Cyprus Current (CC) and the coastal cyclonic flow is called the Asia Minor Current (AMC). Due to the coastal flow and associated instabilities, the AMC is comparable to the AC and the TC (Amitai et al., 2010; Verma et al., 2024). This later flows along the slope until the Turkish coast and back to the Cretan passage.

Within the Levantine Basin we find three major permanent or semi-permanent gyres, described hereafter (Verma et al., 2024).

First, the Mersa-Matruh Gyre (MMG) is an anticyclonic gyre that is centered between 28 and 31°E and between 33 and 34°N depending on the source (Baaklini et al., 2022; Verma et al., 2024; Zodiatis et al., 2023). Its presence is reported in every research while its location is still under debate.

Following, the Cyprus eddies is an eddy/gyre system that is situated at the south of Cyprus, first identified by Brenner (1989) and described by several papers in the recent literature e.g. Egorova et al. (2022); Zodiatis et al. (2023). These vortices reported as "relatively permanent" by Egorova et al. (2022), have a significant impact on the local biogeochemical variables, due to the vertical movement induced by cyclonic and anticyclonic eddies.

Further on the AMC, we find the largest gyre of the eastern basin, called the Rhode Gyre (RG), which flows cyclonically from 28°E to 30°/32°E depending on its size. Ciappa (2021) assessed its importance to trigger the LEC with input of cold water brought by its cyclonic circulation.

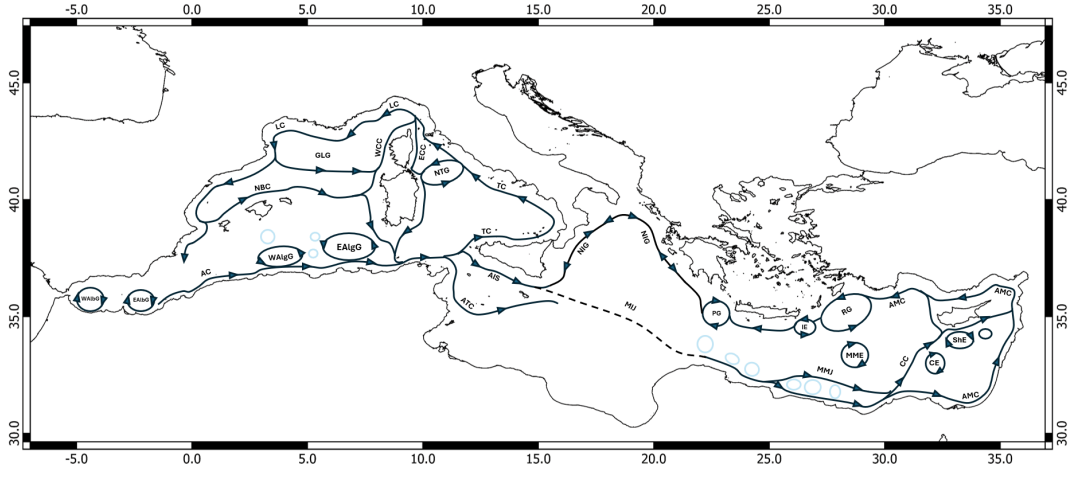

Figure 1. Summary of the literature review. Adapted from <Renault et al. (2012); Soto-Navarro et al. (2010); Testor et al. (2005); Mallil et al. (2022); Poulain (2012); Cotroneo et al. (2016); Pessini et al. (2018); Iacono et al. (2013, 2021); Carret et al. (2023); Pinardi et al. (2015); Poulain et al. (2013); Vargas-Yáñez et al. (2023); Juza et al. (2025); Jebri et al. (2016); Jouini et al. (2016); Martínez et al. (2024); Menna et al. (2019b, a); Napolitano et al. (2025); Borzelli et al. (2009); Liu et al. (2022); Meli (2024); Mkhinini et al. (2014); Civitarese et al. (2023); Baaklini et al. (2022); Alhammoud et al. (2005); Ciappa (2021); Amitai et al. (2010); Verma et al. (2024)>. Dashed line represents the shadow zone corresponding to the literature review and the light blue circles represents the generation of eddies and meso-scale gyres

https://doi.org/10.5194/egusphere-2026-1627
Preprint. Discussion started: 9 April 2026

3 Material and Methods

3.1 Data

The following datasets are used for their surface currents measurements within the Mediterranean Sea. They will be interpolated with DIVAnd method to reconstruct nine years of surface currents at the basin scale.

The HF Radar, drifters, and altimetry datasets were all retrieved from the Copernicus Marine Service (CMEMS) covering the period 2013–2021. The datasets only retain Mediterranean Sea observations. As they did not share the same spatial and temporal resolutions, pre-processing was necessary. For this reason, they were all averaged over a day in order to make them comparable for the interpolation framework.

For the drifters and the HF Radars, the following CMEMS product is used: Global Ocean-Delayed Mode in-situ Observations of surface and sub-surface ocean currents (European Union-Copernicus Marine Service, 2018). The altimetry product is European Seas Along Track L 3 Sea Surface Heights Reprocessed 1993 Ongoing Tailored For Data Assimilation (European Union-Copernicus Marine Service, 2021)

3.1.1 Drifters

710 drifters tracks were used, counting for 465701 observations in the basin for the whole period which count at maximum 1000 observations per region of 30 km^2 (figure 2a). They are transported with the 15 m depth current which will be considered as surface current within this research as Dohan et al. (2010) and Lumpkin and Pazos (2007) have shown to be valid. The velocities are given every 6 hours, which we averaged per day. We isolated a subset of these drifters, taking 25% out of the computation for validation purposes. We note that the Tyrrhenian Sea and the Tunisian coastline are less sampled compared to the remaining part of the sea. In another hand, the Aegean and the Adriatic Sea are not sampled by drifters, except for a few of them that were trapped in the southern Adriatic gyre (Figure 2). Due to this poor sampling, the surface currents won't be discussed for these two regions.

3.1.2 High Frequency Radars

HF Radars are situated in the western part of the Mediterranean Sea at the following locations: At the Strait of Gibraltar, on the Ibiza Island, on the at the Ebro river delta, and at the Gulf of Genoa (Figure 2). It is important to note that the Gibraltar and the Ibiza HF Radars have available observations for the whole period (2013-2021) while the Ebro one was launched in 2014 and the Ligurian one in 2016. Their utility is at measuring coastal flows where altimetry is not accurate. These datasets were available at hourly time step. We decided to take the first observation of the day (at midnight) which are further averaged within each time step. The space resolution is conserved, since the of the regridding of the observations is part of the framework of DIVAnd.

https://doi.org/10.5194/egusphere-2026-1627
Preprint. Discussion started: 9 April 2026

3.1.3 Altimetry

The altimetry dataset represents the main input for observation count. Contrary to the two previous sets of data, the altimetry measurements cover the whole basin for each year of the computed period (Figure 2). The product is processed by DUACS and contains a bundle of satellites, which ensure a large data coverage over the Mediterranean Sea. It includes e.g. Sentinel-6A, Jason-3, Sentinel-3A, Sentinel-3B, Saral/AltiKa, Cryosat-2, Jason-1, Jason-2, among others. Since the product gives daily information of the surface altimetry, temporal processing of the data was not needed. The measure of altimetry is used as a proxy to compute the pressure gradient. This pressure gradient is then used to compute the associated surface velocities through the geostrophic equilibrium. This latter is known to be a reasonable approximation whenever the field is characterized by low Rossby and Ekman numbers, respectively low contribution from inertial forces and low contribution from the fluid viscosity (Beckers and Cushman-Roisin, 2011).

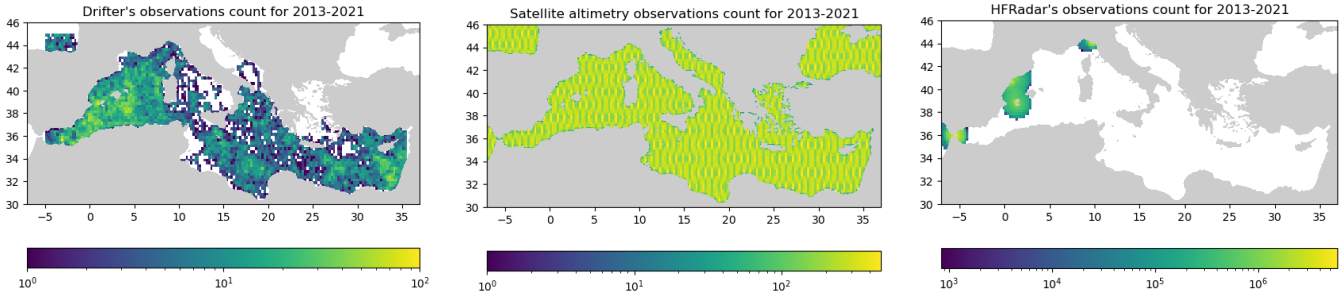

(a) Drifter data (b) Satellite data (c) High Frequency Radar data

Figure 2. Spatial coverage of the different dataset used for this study.

3.2 DIVAnd

DIVAnd is a multivariable interpolation method. It was originally described in Brasseur and Haus (1991) and later presented as a univariable inteprolation method by Troupin et al. (2010). Based on these work a multivariable interpolation method was developed by Barth et al. (2014) which were adapted for surface currents in Barth et al. (2021). Therefore based on a cost function, it computes a scalar variable $J(\phi)$ that depends on the difference between the variable $\phi(x_j)$, the observations d_j and the spatial/temporal regularity of the field.

$$J(\phi) = \sum_{j=1}^{N_d} u_j \left[d_j - \phi(x_j)\right]^2 + |\phi - \phi_b|^2 \tag{1}$$

In this cost function, ϕ is the ocean field and N_d is the number of observations for the locations x_j, ϕ_b is the background estimate which is a first guess of the interpolated field, (here ϕ_b is set to zero) and the spatial/temporal regularity is defined using the following norm:

https://doi.org/10.5194/egusphere-2026-1627
Preprint. Discussion started: 9 April 2026

$$|\phi|^2 = \int_{\Omega} \left(\alpha_2 \left(\nabla^2 \phi\right)^2 + \alpha_1 \left(\nabla \phi\right)^2 + \alpha_0 \, \phi^2 \right) \mathrm{d}\Omega \tag{2}$$

where ∇ is the gradient operator and ∇^2 is the Laplacian of the field (equation 2). For the variational inverse method, any physical laws or other constraint can be added as additional terms to the cost function (equation 1). More information about the mathematical formulation of these physical laws are described in Barth et al. (2021). In our work, two constraints out of four will be used; The coastline effect (equation 3) and the divergence constraint (equation 4).

$$\mathrm{u} \cdot \mathrm{n} \sim 0 \tag{3}$$

Where u is the velocity adjacent to the coastline and n is the vector normal to the coastline. Second, we added a divergence constraint which says that at any point of the reconstructed field, the horizontal flux for every grid cell must be balanced.

$$\nabla \cdot \mathbf{u} \sim 0 \tag{4}$$

For each time instance, corresponding to one month, we gather the corresponding observations, and we interpolate them, excluding the validation drifters. As explained earlier with the equations 1 and 2, DIVAnd computes the field that match the best the observations while being the smoothest possible, taking into account the coastline and the divergence constraint. There the reconstruction is evaluated by comparing the corresponding independent observations to the newly reconstructed field. The validation is further described in the section 3.4.

3.3 Parametrization

In 2D cases like this one, time correlation is not forced, meaning that each time instance is reconstructed independently. For each of these reconstructions, two free parameters are shaping the result; the correlation length (L) and ϵ^2, error variance of the observations (normalized by the error variance of the first guess).

First, the correlation length is proportional to the scale of the interpolated domain. The largest it is, the further the observations will have an influence on the reconstructed field. Second, the error variance of the observations is a parameter that is related to the accuracy of the observations. The smaller this number is, the larger the confidence will be given to a data point. In this case, we decided to associate three different errors variances; respectively for the drifters, the satellites and the HF Radar observations.

The grid size of the result is fixed to 1/4° in both directions (along the meridional and zonal component) which corresponds to a latitude extent of 27.75 km resolution while the longitudinal extent is on average equal to 18.2 km with 49° as a latitude average. This resolution was selected because it represents a compromise between the computation of mesoscale processes and

https://doi.org/10.5194/egusphere-2026-1627
Preprint. Discussion started: 9 April 2026

computation time. The time resolution is set to a month. It represents an outstanding compromise as we have to gather enough observations to accurately reconstruct the field and to compute the seasonal and monthly variations.

3.4 Validation

For the validation, we decided to do a cross validation using drifters. The choice of the drifters as a dataset source for validation is coherent since they are the only in-situ measurement of the study and therefore, are considered as the most reliable observations (Poje et al., 2014). Moreover, they have a reasonable cover for the considered period (figure 2a). To do so, we assigned to each drifter a number (Drifter ID) and we randomly selected in space and time a subset of these IDs, representing 25% of their total amount. Doing this ensures to not split a drifter trajectory by retrieving their complete path. This subset was not used for the interpolation and was rather kept aside for its comparison to the results, which assess the interpolation accuracy. Once retrieved, we linearly interpolated the result onto the validation drifters positions to compare both. The interpolation results are monthly averages, therefore, the validation drifters will gather a month of observations. The validation is based on the "Root Mean Squared Error"(RMSE) (equation 5) and the correlation at each month for u and v velocities.

In the equation 5, n represents the amount of independent observations gathered each month (on average 34 observations per month for 2021), $\hat{y}_i$ represents the prediction of DIVAnd linearly interpolated on the position of the observation y_i. Thus, an RMS error is computed for each month, with varying position among the domain.

$$\text{RMSE} = \sqrt{\frac{1}{n}\sum_{i=1}^{n}(y_i - \hat{y}_i)^2} \tag{5}$$

The optimization of the two free parameters (here correlation length and signal-to-noise ratio) were carried out with "Julia Black Box Optim", a package that sets random values (in a given range) for both parameters and are optimized based on the RMS. We sought parameters values that minimize the RMS error for a year of computation. The values leading to the lowest RMS error were kept. Once found, these values were kept for any year of the analysis (from Jan 2013 to Dec 2021). As a double check for the interpolation accuracy, other years were validated with the remaining independent observations.

4 Results

4.1 Validation

The validation of the results is performed in the year 2021 for its great data coverage, where we gathered 409 independent observations from surface drifters and compared them to the DIVAnd method, and later, to the DUACS product. For each month, the meridional and zonal components of the velocity were compared to independent observations using the RMS Error (equation 5).

https://doi.org/10.5194/egusphere-2026-1627
Preprint. Discussion started: 9 April 2026

4.1.1 Parameter value

The following parameters values L and ϵ^2 are found (table 2). The correlation length obtained is 137,80 km. The error variance of the observations has three values; one for each source of the dataset.

/	Parameter value
Correlation length	137.8 km
ϵ Altimetry	0.026
ϵ Drifters	0.006
ϵ HF Radars	0.098

Table 2. List of hyperparameters tuned for the analysis based on the validation. The correlation length is given in kilometers and the epsilon parameter is an error ratio.

First, as expected, drifters are found to be the most reliable source of observations as the validation is performed with the same tool and their measurment is in-situ. The speed derived from altimetry has a higher error compared to the drifters, which is due to the assumptions made to derive the speed from water elevation. Finally, HF Radars are found to have the highest error variance among the three source of observations, which can be explained by the redundant observations within radars. Indeed, whenever two observations are closely correlated, the error variance is increased for computational facilities, which has the consequence of reducing their use and, therefore, to increase the error variance. This phenomenon is depicted in Lee and Song (2017) for the interested reader.

A graphical example of the validation is shown in figure 3 for June and December. In both examples, the validation drifters are located in the eastern part of the Mediterranean Sea. The June drifter (figure 3a) is trapped in the well-known Cyprus eddies where it follows the streamlines computed by the interpolation. The December one (figure 3b) is following the Asia Minor current, where its velocity rises along the south-eastern boundary of the sea and reaches speeds up to 0.5 m/s. The RMSE for June is 0.045 m/s for the meridional velocity (u) and 0.042 m/s for the zonal velocity (v). The error for December is equal to 0.072 m/s for the meridional velocities (u) and 0.029 m/s for the zonal velocities (v) which are the months with the smallest RMSE in 2021. Within the validation year, the largest RMSE is found in February (figure 6).

We aimed to compare the entire year of independent observations with the reconstructed results, rather than solely having a month-by-month visual comparison. To this end, the velocities were separated into their zonal and meridional components and plotted in a scatter plot, from which were derived regression lines. The ideal slope (where the independent drifters are exactly the same as the results) would have a slope equal to one and the intercept equal to zero. These results are shown on figure 4.

It is found that the independent observations and the results are equivalent in both directions, having a slope equal to 1.34 for the meridional velocities and equal to 1.28 for the zonal velocities and intercept equal to 0.01 and 0.05 respectively. We can see that there is higher variability with their zonal component of the velocity compared to the meridional one. This could be easily explained due to the inner circulation properties of the Mediterranean Sea for which the major stable flows are found along the

https://doi.org/10.5194/egusphere-2026-1627
Preprint. Discussion started: 9 April 2026

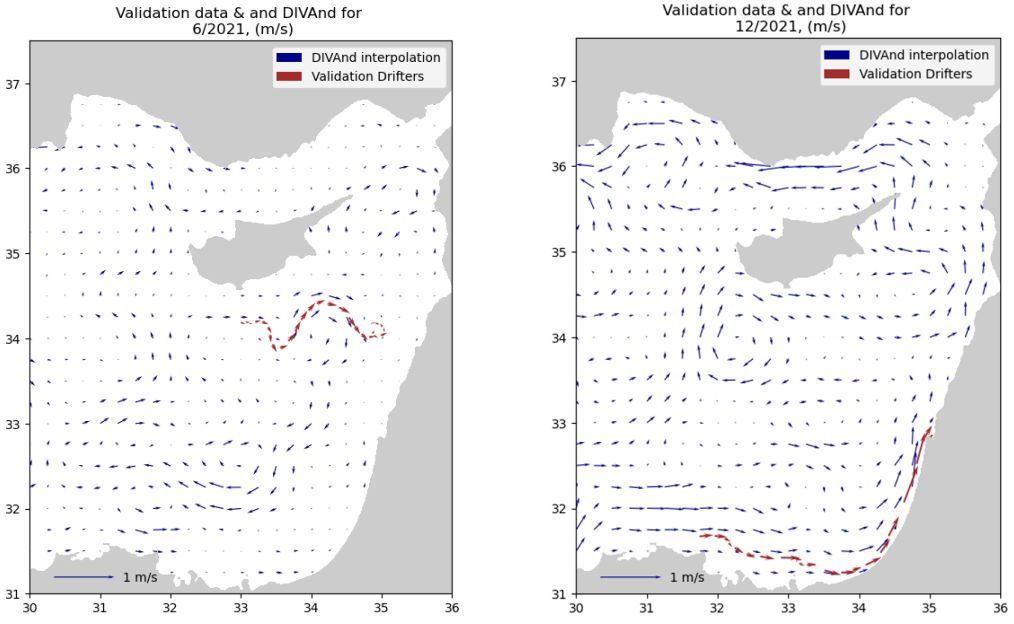

(a) (b)

Figure 3. Two months examples of the validation for DIVAnd results. Red arrows represent the velocity of independent drifters and the blue arrows are the results of DIVAnd interpolation computed with a resolution of 1/4°.

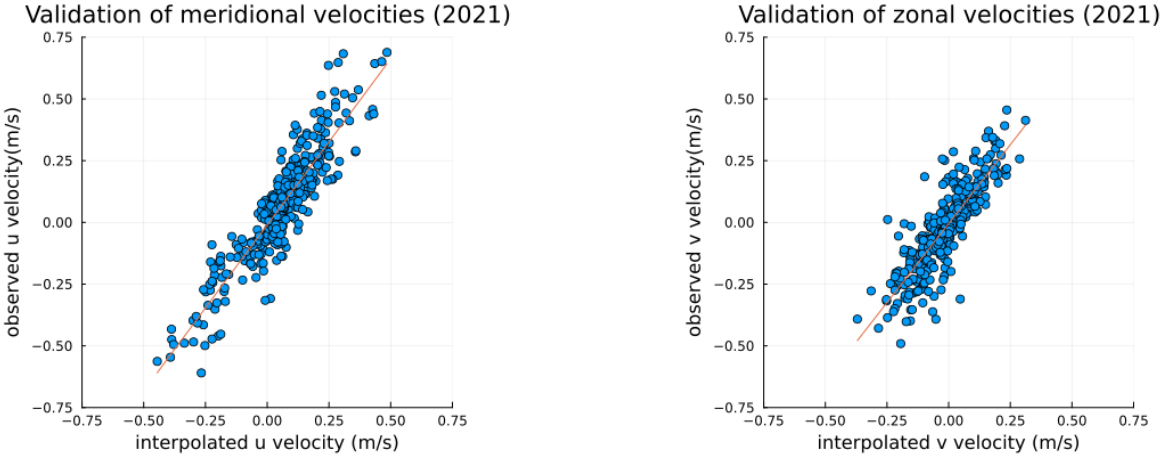

(a) (b)

Figure 4. Linear regression and scatter comparison of the two components of the velocity (meridional and zonal) with the independent observations for the year 2021.

https://doi.org/10.5194/egusphere-2026-1627
Preprint. Discussion started: 9 April 2026

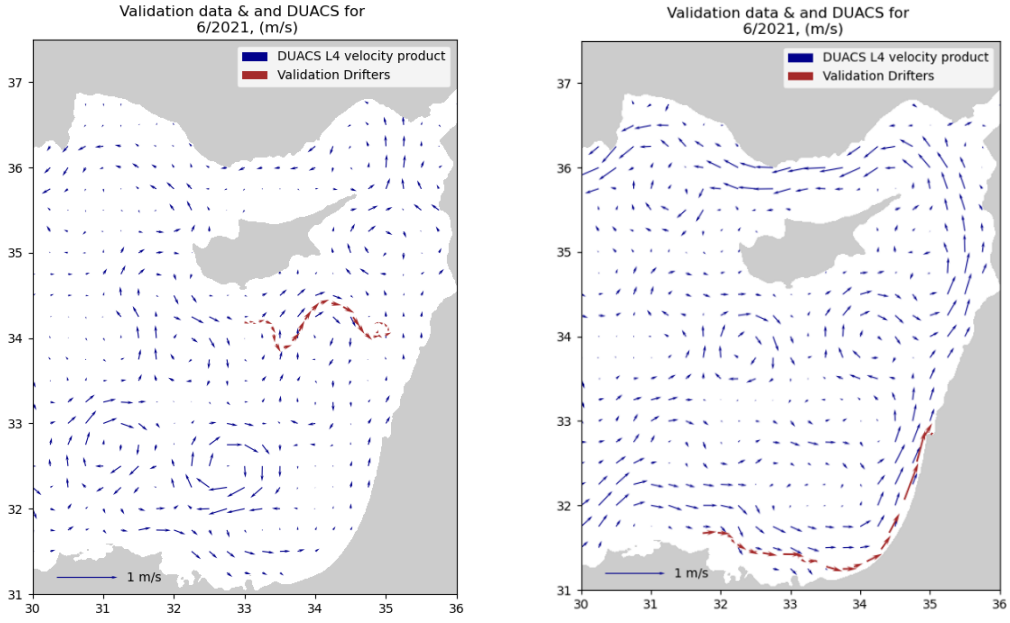

Figure 5. Two months examples of DUACS comparison with independent drifters. Those products were processed by SSALTO/DUACS and distributed by AVISO+ (https://www.aviso.altimetry.fr) with support from CNES.

coast and therefore, in majority, along the meridional direction. Thus, it is normal to find higher variability along the zonal axis. Moreover, we find both of the regression slopes up to one, which means that on average, the independent drifters have higher velocities compared to the interpolation results. This could be explained by two different reasons. First, we compare monthly averages to instantaneous velocities, making the drifter's velocities likely to be larger. Second, DIVAnd smooths the field to create the interpolation, which reduces the highest velocities while the independent drifters keep their high ranges. Therefore, we will always find higher independent velocities compared to interpolation results. We note that the slope is slightly higher for the meridional velocities, meaning that the meridional velocities show a greater degree of underestimation compared to the zonal velocities.

4.2 Comparison with geostrophic velocities from DUACS

Since our surface currents are also derived from drifters and HF Radar, rather than solely from altimetry, we assume that our results should capture processes beyond geostrophic dynamics. This would allow us to analyze smaller-scale features characterized by higher variability and increased precisions for instabilities, which are abundant in the Mediterranean Sea (Baaklini et al., 2021). Therefore, a comparison with geostrophic products is performed to confirm our hypothesis (Copernicus Marine Service, 2023). To this end, we carried out a validation procedure using the same independent drifters as on the main

https://doi.org/10.5194/egusphere-2026-1627
Preprint. Discussion started: 9 April 2026

results for the geostrophic velocities (Figure 5). In order to make both results comparable on their temporal extent, we decided to average the geostrophic velocities per month. The resulting RMS error is reported in Figure 6.

On average, the computed RMS errors with the DUACS product over the year 2021 are higher compared to the DIVAnd interpolation. Indeed, they count 0.138 m/s for the meridional component and 0.119 m/s for the zonal component of the velocity, while the RMS error for the DIVAnd product corresponds to 0.095 and 0.082 m/s respectively.

This last result demonstrates that the contribution of drifters, HF radars, and the imposed physical constraints of the method enables the resolution of surface currents with high accuracy at the monthly scale, beyond geostrophic dynamics. These results are therefore valuable for analysing seasonal patterns and specific dynamics over nine years of observations.

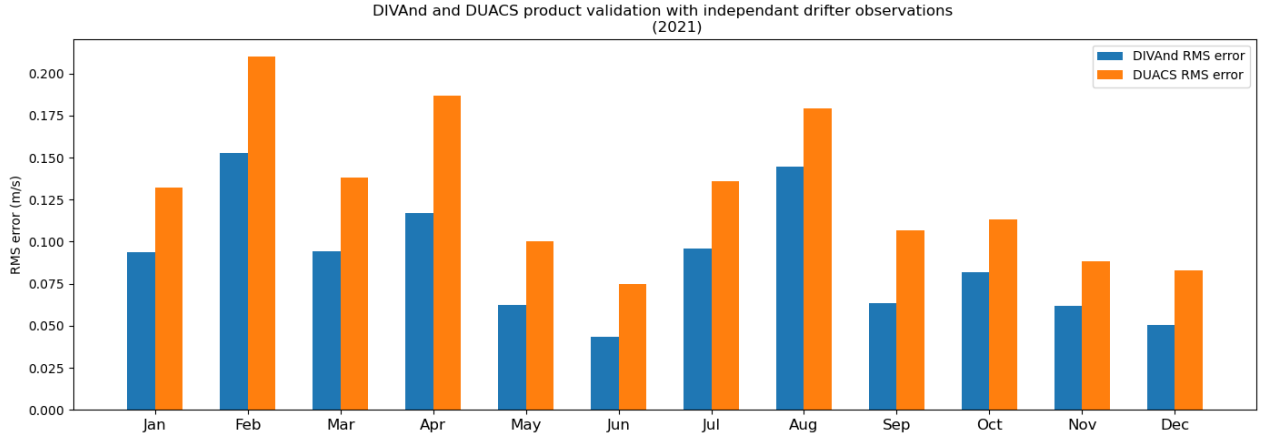

Figure 6. Comparison of the monthly averaged DUACS L4 surface currents and DIVAnd interpolation results RMS error based on independent drifters observations.

4.3 Seasonal variation with climatic averages per month of 2021

First, the present paper will discuss the seasonality of the major known currents in the Mediterranean Sea: Alboran Gyres, Algerian Current, Tyrrhenian Current, Northern Current, Sicily Channel dynamics, Lybio-Egyptian Current, Asia Minor Current and the major gyres of the eastern basin. Their seasonality will be shown based on climatic averages for the winter-summer differences occurring in the 2013-2021 period (figure 7). To do so, the currents were averaged in June, July and August for the summer period and in December, January and February for the winter period. These averages will highlight the most consistent features at the seasonal scale for the considered period.

https://doi.org/10.5194/egusphere-2026-1627
Preprint. Discussion started: 9 April 2026

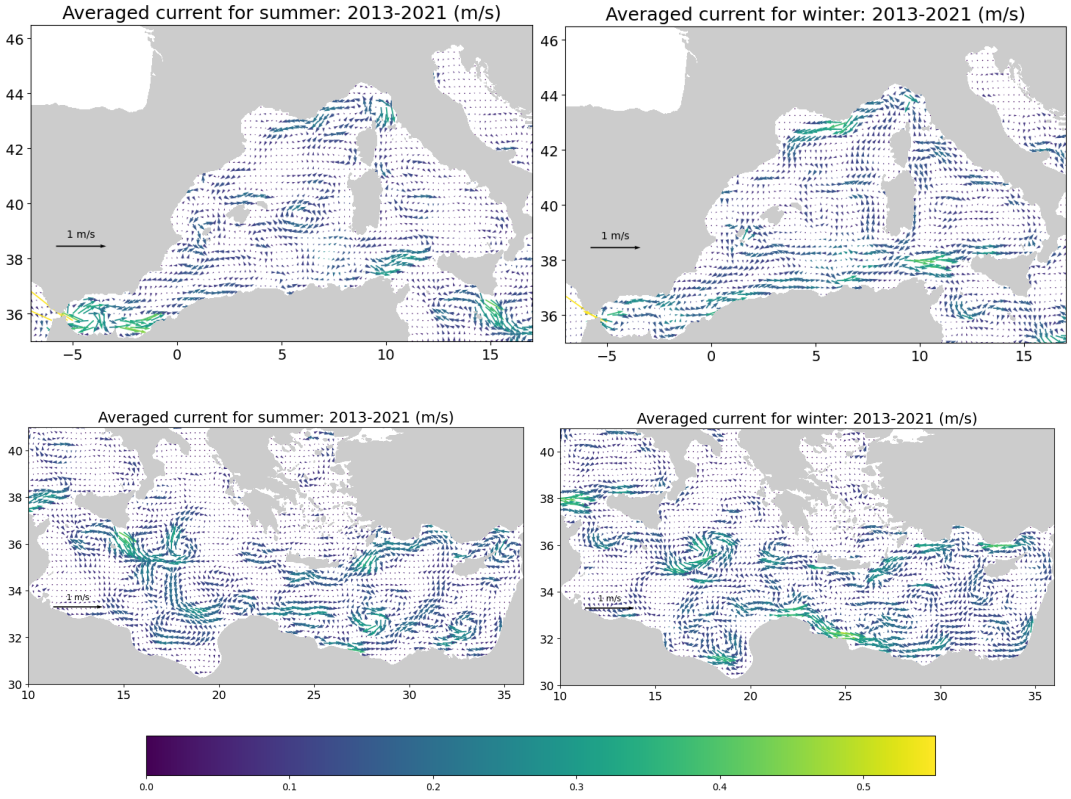

Figure 7. Seasonal averages for summer (June to September) and winter (December to February) at the basin scale. Averages are computed for 2013–2021.

Alboran Sea

First, in the Alboran Sea, the Western Alboran Gyre (WAlbG) is stronger and better defined in summer (centered around -4.5°E, 36°N), with a current speed up to 0.4 m/s in the climatology and up to 0.55m/s in spontaneous results. This gyre sets as an anticyclonic gyre at the end of spring and lasts until October, which agrees with (Renault et al., 2012). During winter, the presence of the WAlbG is less consistent, which prevents its emergence in the decadal-scale analysis. However, the WAlbG rarely disappears for more than two months. The Center Alboran Gyre and the Eastern Alboran Gyres are not consistent enough neither in winter nor in summer to be captured on these averages, which confirms the dominance of the WAlbG. It is important to note that we captured a much more complex circulation in monthly velocities, sometimes composed by 3 or 4 gyres at the same moment which brings complexity to the modes observed by Renault et al. (2012). This last conclusion confirms the SSH profiles measured by Brett et al. (2020), highlighting an episodic and complex hydrodynamical circulation. This complex circulation often sets after summer, and disappears with the deepening of the mixed layer.

https://doi.org/10.5194/egusphere-2026-1627
Preprint. Discussion started: 9 April 2026

Algerian Current

The AC is stable from 0°E to 4°E at the climatic scale. We observe slightly higher velocities in winter compared to summer, reaching 0.4 m/s in the climatology. We find the reduction of the current speed (due to enhanced instabilities) covering a larger longitudinal range in summer (4°E to 10°E) compared to winter (from 5°E to 6°E) as shown on figure 7. Indeed, in winter, due to the intensification of the wind speed and the extended mixed layer depth, the AC, which is on average lighter than the Mediterranean water, flows deeper, faster, and therefore, is more stable during the cold season (figure 7, figure 8a). On the other side, the enhanced stratification due to the higher temperature and the overlying of AW over Mediterranean water has a tendency to make the AC unstable and slower during summer, forming a highly variable gyre field from which an example is given figure 8b.

Tyrrhenian Sea

The Tyrrhenian Sea has a strong variation between summer and winter, having a well-defined coastal current during cold months and a highly unstable surface during summer (figure 8c-d). This was first described in Iacono et al. (2013), describing that the surface circulation goes from coastal currents to gyral circulation. These instabilities are thought to be enhanced by the emphasis of the stratification caused by the rising temperature. Transitional states with meanders and baroclinic instabilities are captured at the monthly temporal scale in our results. Our conclusion meets the one brought by Iacono in his papers (Iacono et al., 2013, 2021), and won't be discussed more here.

Liguro-Provencal basin and Balearic Island currents

The NC is observed in both periods between 9°E and 5°E, having higher velocities in winter; up to 0.35m/s, compared to summer; below 0.2 m/s (figure 7). In both seasons, the current decreases its velocity just after crossing the Gulf of Lion as we observe currents around 0.1 m/s. Additionally, the GLG is not clear as its size and location is highly variable with time. However, it is clearly seen on spontaneous results.

Further, at the latitude of the Balearic Islands, during summer, the current turns eastward on the northern side of the archipelago, forming the NBC (around 40°N as mentioned by Vargas-Yáñez et al. (2025)). Meanwhile, in both seasons, a part of the flow tends to pass through the islands toward the Alboran Sea. Although the seasonal mean circulation shows a predominantly southward flow across the Balearic Islands, we also observed a northward current, which caused the Alboran Sea to feed the NBC. This pattern happened 4 times in the considered period; first in winter 2013, once in winter 2016, during summer and autumn 2017 and last, in winter 2021. The drivers of this phenomenon are not known since a physical explanation of the reversal is, to our knowledge, not mentioned within the literature. One hypothesis brought by Vargas-Yáñez et al. (2025)

https://doi.org/10.5194/egusphere-2026-1627
Preprint. Discussion started: 9 April 2026

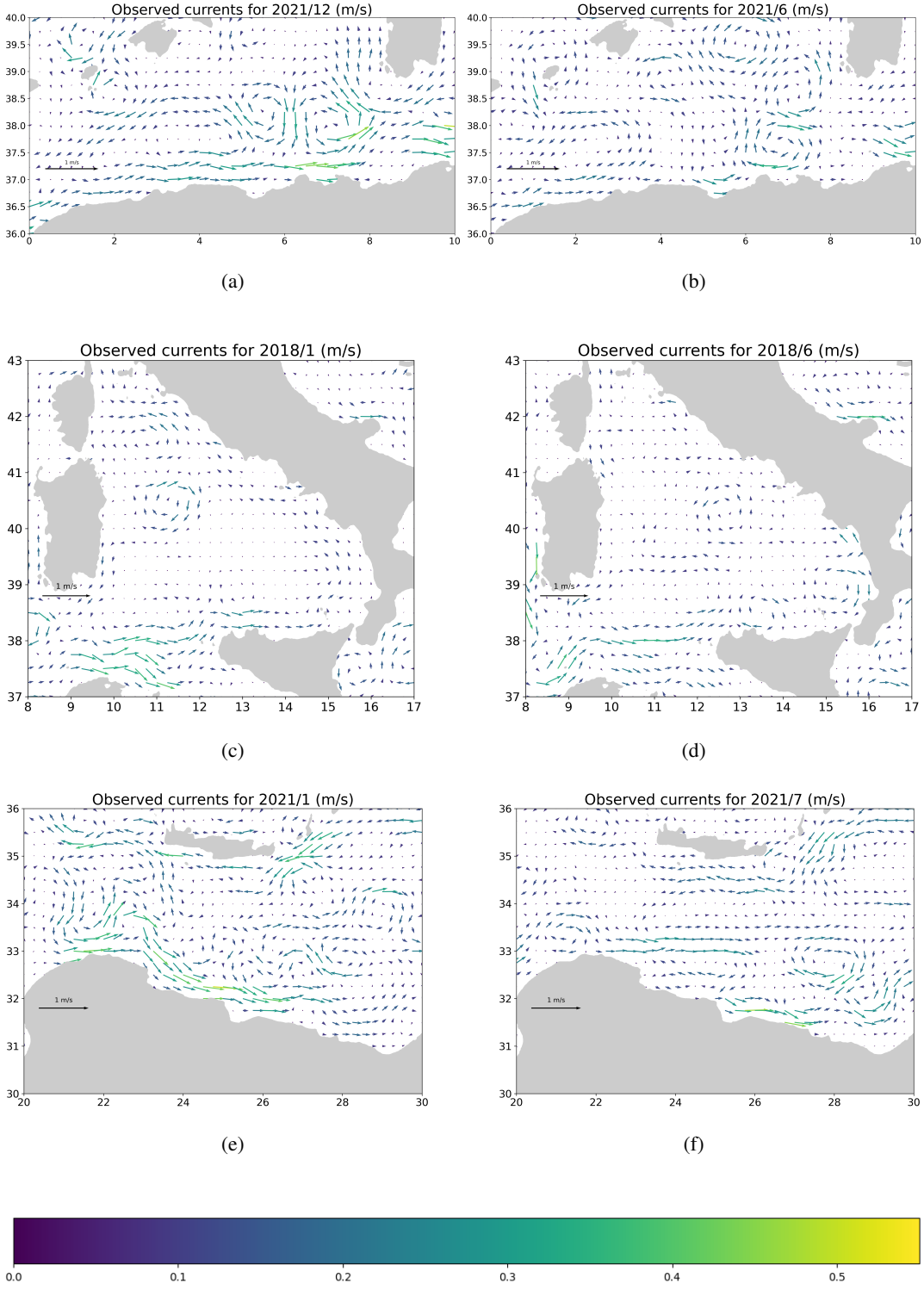

Figure 8. Spontaneous monthly circulation showing the non-stable behavior of summer compared to the deep and stable winter circulation: (a–b) Algerian Current, (c–d) Tyrrhenian Current, and (e–f) Libyo–Egyptian Current.

https://doi.org/10.5194/egusphere-2026-1627
Preprint. Discussion started: 9 April 2026

is that the mesoscale events are strongly influencing the zone, having the potential to sporadically change the circulation. This hypothesis is even stronger as we notice that the northward flow never settles for more than a one-month period.

Sicily Channel, AIS and ATC

The AIS has a remarkable difference between winter and summer; in its velocity and its path. In winter, the large and fast last portion of the AC (around 10°E) induces large transport along the Tunisian continental slope. Indeed, the AIS follows the continental slope from 38°N until 36°N with velocities around 0.2-0.3 m/s (figure 7). Once the current has crossed the Sicily Channel (at 36°N), it is directed to the east, toward the Sicily continental slope where the current gains in velocity (figure 7). The temperature profile with a front separating the southern Ionian waters and the northern AW is the key to explain the winter path within the channel (Jebri et al., 2017). In summer, the current is not flowing along the Tunisian coast nor at the Sicily continental slope and rather has a large and slow path that flows around 0.1 m/s. Nonetheless, the currents still gains in velocity while passing on the Sicily shelve. On its side, the ATC does not display enough consistency to be detected in climatic averages; it is only observed sporadically at the monthly scale, only at the beginning of the period of interest. Its variability, the lack of drifters within the region, combined with low velocity current, are responsible for its low detection with DIVAnd.

Ionian basin

The AIS is known to follow the Sicily continental slope before being directed to the Ionian Sea towards the Cretan passage, there, becoming the MIJ. This jet is known to have a high temporal variability and to be surrounded by many vortices (Mkhinini et al., 2014). The pathway of the MIJ has often been described in the literature as a simple forward trajectory within the Ionian Sea (e.g., Pinardi et al. (2015); Menna et al. (2019b); Liu et al. (2022); Civitarese et al. (2023)), as it is in our results for the 2013–2019 period and particularly during summer (Figure 9a). However, the results corresponding to 2020 and 2021, report a complex and relatively stable circulation, where the MIJ crosses twin vortices (figure 9b) located at 36°N and around 16°E and 18°E each (cyclonic and anticyclonic from west to east). These two vortices shape the path of the MIJ, influencing the current, the temperature and the biogeochemistry of the central Ionian basin as it is stable for months (figure 10). This last result shed light on a transition between two modes of circulation both shown on figure 9. These gyres are associated with a frontal zone between the warm waters of the southern Ionian and the colder, fresher waters of the Adriatic Sea, which can be identified in temperature maps (figure 10). After crossing the twin gyres, the MIJ is directed southward, creating cold water intrusions at the southern part of the Ionian Sea (figure 10a-f). Then, the flow will turn eastward to join the northernmost part of Libya, which will create the Lybio-Egyptian Current.

We note that during both periods, we find a northward current on the west side of the MIJ which starts at 15°E-33°N and ends at 12°E-36°N. This location was not expected to be the location of a northward current as the ATC settle there. To our knowledge, this counter-current has never been reported in the literature (figure 7,9).

https://doi.org/10.5194/egusphere-2026-1627
Preprint. Discussion started: 9 April 2026

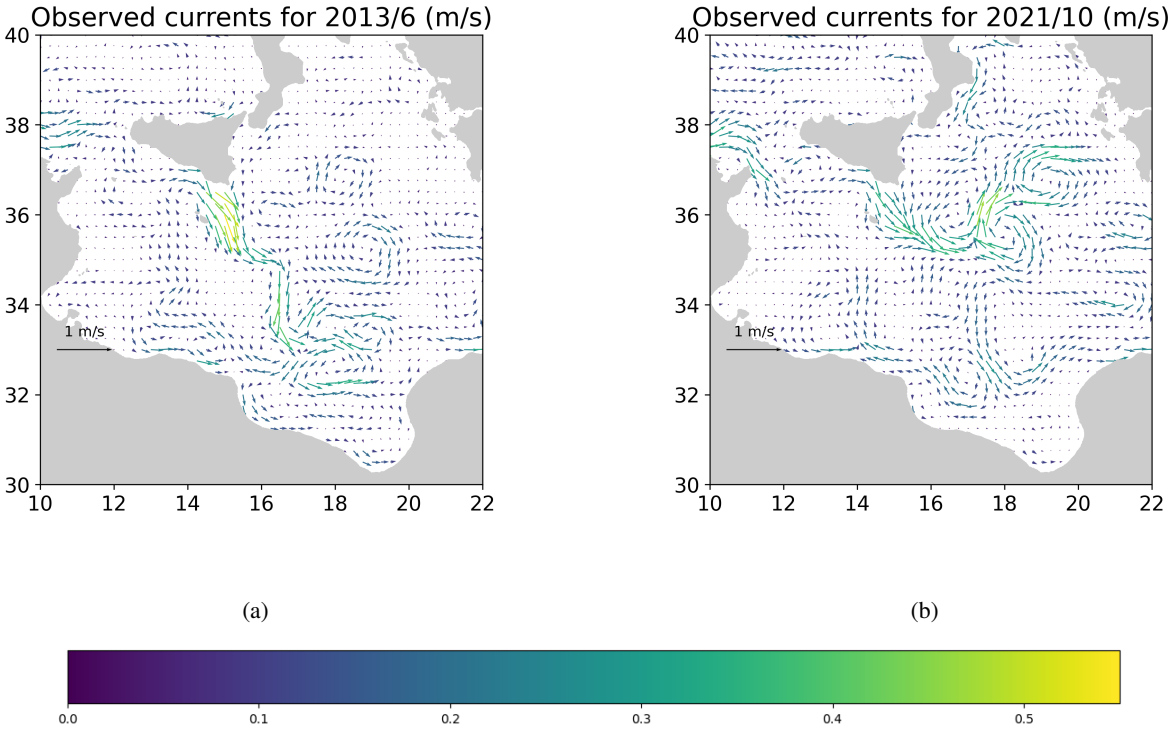

Figure 9. Comparison of two modes of circulation observed in the central Ionian Basin.

Cretan Passage and Levantine basin

The LEC is the strongest and the fastest current of the averaged seasons (figure 7). It starts at 21°E-33°N at the coast of Libya, fed by the MIJ (no matter its path in the Ionian Sea), and flows south-eastward (along the coast) during winter while flowing purely eastward in summer, detaching from the coast, due to the presence of anti-cyclonic gyres (figure 8e). These conclusions were already given by Ciappa et al. 2021 and our results act here as a confirmation as the phenomenon is observed on long time averages (figure 7). Further, around 27°E, the LEC is separated in two branches, one following the coast and the other one flowing seaward to join Cyprus Island. The branch flowing seaward is the CC and is detected in both seasons on the same path, being wider in winter than in summer (figure 7). The branch flowing along the coast is named AMC. This latter undergoes significant instabilities populated by gyres and eddies in both seasons, making the AMC almost invisible, especially at the summer climatic scale. With the yearly warm up, the amount of mesoscale activities along the coast increase, having a comparable seasonality with the TC. Therefore, during summer, on large temporal averages, the CC becomes the only one found in the Levantine basin, the rest of the region being populated by mesoscale eddies, not captured here at the climatic scales (figure 7). Further, during winter, the AMC is more stable compared to summer, making it clearer on the results (figure 7). However, a region situated between 33°N and 36°N on the eastern border of the basin remains highly turbulent during the cold season, where the AMC does not have a clear path at the climatic scale. This last sentence supports the results of Verma et al. (2024).

https://doi.org/10.5194/egusphere-2026-1627
Preprint. Discussion started: 9 April 2026

Futher along the coast, the AMC merge with the CC nearby Turkey and flow westward, back to the Cretan passage and to the Ionian basin.

The end of this section will describe the permanent and semi-permanent gyres that are reported in the introduction, known as MMG, CE, RG.

First, the anti-cyclonic MMG is spotted in both seasons, making it consistent on the whole period. It is situated westward of the bifurcation of the LEC, centered at 27.5°E-33°N. This gyre is better defined in summer and has speed reaching 0.4 m/s while winter averages are closer to 0.1 m/s.

In the south of Cyprus island, we spot a semi-permanent eddy, centered at 32.5°N-32.5°E. This last is part of the CE system. It is well-seen in summer, while its presence in winter is unclear, as the climatic average does not retain its complete signature. Indeed, the coastal current (AMC) overlaps the gyre during winter as it grows in speed and space (figure 7). This gyre is the only gyre spotted on climatic averages from the Cyprus Eddies system depicted in the introduction.

Further, the Rhode Gyre is not seen on the averages. The last part of the AMC (that flows from 30°E to 27°E and around 35°N), is the northern part of the RG, and is well-defined all year long while the southern part of the gyre is not observed on long term averages. However, it is observed sporadically on spontaneous results and follows properly cold water intrusion, observed with satellites.

4.4 Twin Gyres and the Ionian front

We decided to shed light on the central basin of the Ionian Sea in the context of the complex BIOS system (Civitarese et al., 2023). Indeed, several researches were carried to understand the reversal of the NIG and its physical insight e.g. (Kalimeris and Kassis, 2020; Borzelli et al., 2009; Liu et al., 2022; Meli, 2024) while the surface current of the central Ionian Sea is only poorly understood. Our results show a clear transition within the circulation of the central Ionian Sea going from a simple forward path before 2016 to the amplification of a gyral complex circulation from 2020 to the end of our period of interest (figure 9).

First, we verified that this pattern does not result from an interpolation artifact. To do so, we compared the surface current to the temperature patterns measured by satellite. The product is referred as Copernicus Climate Change Service and Collecte Localisation Satellites (2021) and exampled with the figure 10a-f. These examples show that the streamlines does not result from an interpolation artifact as the currents follows rigorously the temperature isotherms.

We first remark that a front is systematically observed when the TGs are present. This later is positioned as an extension of the Sicily continental slope, at the beginning of the MIJ (approx. 16°E-36°N). This front is the result of the cross-road between the cold AW coming from the SC, the Adriatic cold water intrusion and the hot southern water of the Ionian Sea. This front does not only separate southern and northern water but is also shaped by the presence of the TGs as we see hot water intrusion at 18°E-36°N and cold water intrusion around 16°E-36°N, corresponding to the location of the gyres computed with DIVAnd

https://doi.org/10.5194/egusphere-2026-1627
Preprint. Discussion started: 9 April 2026

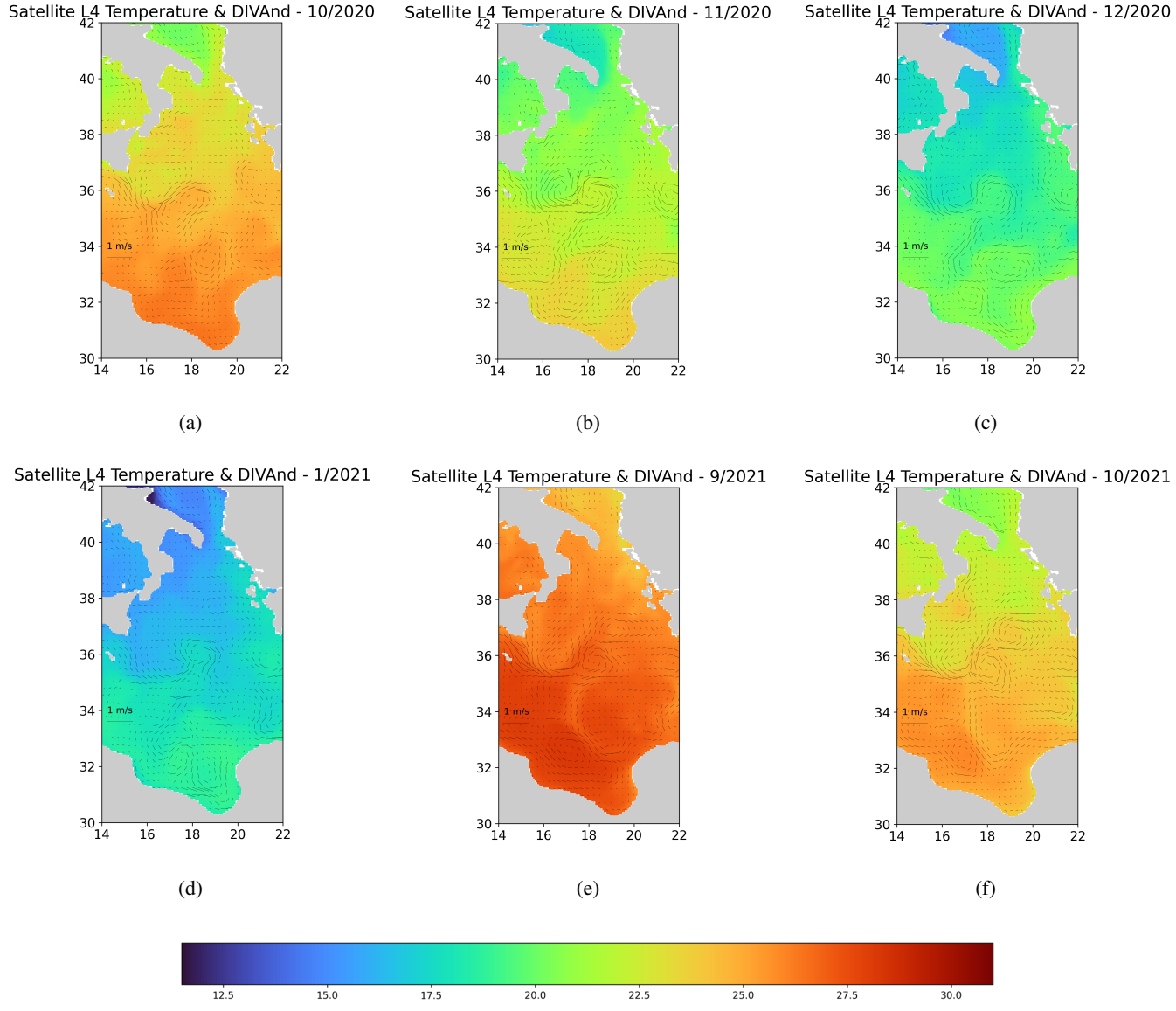

Figure 10. Twin Gyres examples: Surface currents superposed with L4 satellite temperature (°C) for the period 2020 - 2021

(figure 10a-f).

In order to highlight the appearance of the TGs and the associated mechanisms, we decomposed the Ionian Sea (corresponding to 108 months of the DIVAnd result) into modes with orthogonal functions. Using a singular value decomposition (SVD), the first mode explains the most variability and the last explains the less. To highlight solely the circulation patterns of the Ionian Sea, we selected a spatial subset of the results, corresponding to 13-23°E and 34-40°N as it is on figure 11a. This was

https://doi.org/10.5194/egusphere-2026-1627
Preprint. Discussion started: 9 April 2026

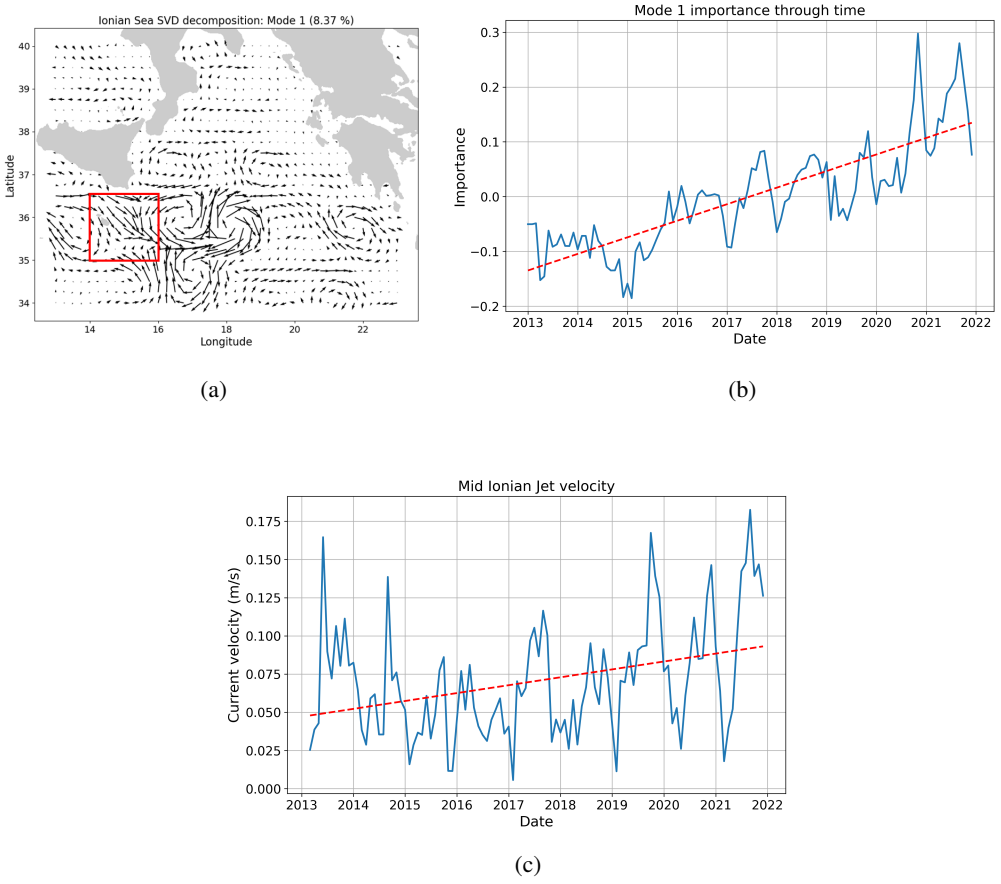

(a) (b)

(c)

Figure 11. Ionian Sea SVD decomposition: first mode in space and time. Measured speed along current and Mid Ionian Jet averaged velocity

performed with the package "LinearInterpolation" in Julia language.

The TGs appear in the first mode (figure 11a) which explains 8.37% of the variability of the Ionian Sea for the whole period and exlplains 30% of the variability at the end of 2020. This mode emerged in 2017 and appeared every following year, growing steadily over the considered time period (figure 11b). It emerges with a distinct seasonality, being always stronger in the second half of the year, (around autumn/early winter) and peaking at the end of 2020, showing its rising importance.

As the gyres seem to be stable for months and were already seen in previous year (figure 9a), we could suspect the enhancement of pre-existent gyres due to the changing path of the MIJ. We also suspect the NIG to play a role in this phenomenon, being responsible for the strength of the MIJ as Menna et al. (2019) demonstrated. To answer the question, we will rely on the SVD results, which will highlight patterns concomitant with the appearance of the TGs.

As shown on figure 11a, it suggests that the TGs are highly correlated to the AIS input as the end of the AIS and the beginning of the MIJ is well represented on figure 11 (red square). On the other side, the rotational direction of the NIG does not

https://doi.org/10.5194/egusphere-2026-1627
Preprint. Discussion started: 9 April 2026

seem to be an important factor as it is not seen on the same mode.

Following this last conclusion, we averaged the monthly AIS speed over the considered period (2013-2021). To do so, we defined a spatial subset represented by the red square and computed the velocity and direction averages considering every month (figure 11a). From these results, a new axis system was established aligned with the principal direction of current variability. The monthly mean velocity associated with this system is reported in Figure 11c.

We first remark that the maximum speed in winter rose for the last 6 years of the period, while the lowest speed in summer almost stayed the same. The transitions between summer and winter are thus more and more abrupt, creating a positive trend of the speed over the period. The both winter intensification of the MIJ and the TGs are concomitant and support the first hypothesis linking the MIJ speed and the appearance of the TGs. However, the velocity of the AIS cannot explain alone the appearance of the TGs as these velocities were already reached without inducing this pattern.

A reasonable cause could be the intensification of the Ionian temperature gradient, enhancing the observed front, which encourages the current in the direction of the pre-existent gyres, creating the TGs. In these conditions, the intensification of the AIS followed by the intensification of the front would induce the enhancement of stable and strong TGs which remain present during winter time.

These have the consequences to modify the physical properties of the central Ionian Sea as it modify the temperature and the currents profiles. Consequences cannot be yet measured, but these modifications will have consequences on the Mid-Ionian Sea seasonality. Modifications on the mixed layer depth, chemical components and biological productivity are expected.

5 Conclusion

In this paper, we interpolated and validated at a monthly scale Mediterranean Sea surface currents. To do so, we used the interpolation method DIVAnd with which we mapped nine years of surface currents from three different sources of observations: drifters, altimetry, and HF Radars. These results were validated against independent drifters and compared to geostrophic surface current estimates that use only altimetry. The validation showed significant agreement between the independent drifters and the calculated results per DIVAnd. We carried out the same validation with DUACS velocities and showed the improvement brought by the additional data and the dynamical information used in the analysis (imposed physical laws: equation 3 & 4). Indeed, we obtained a higher error with the geostrophic product (figure 5), which we observe to be less variable than our results (figure 3 versus figure 5). Furthermore, the validation procedure shaped the parametrization, showing that the in-situ measurements were the most reliable, followed by the satellite measurements, while HF Radar have the highest error variance, explained by the redundancies of the dataset (Lee and Song, 2017).

At the basin scale, our study highlights the coastal to gyral circulation as the major change in the Mediterranean basin for the winter to summer variation. In our observations, we could example the increased amount of gyres during summer with the WAlbG, the Tyrrhenian Sea, the LEC, the MME and the CE southern gyre. On the winter side, we mainly observed the coastal

https://doi.org/10.5194/egusphere-2026-1627
Preprint. Discussion started: 9 April 2026

currents to be better defined and more stable. The AC, the TC, the LEC and the AMC are the main examples to highlight this phenomenon. Concretes examples of seasonal transitions are shown on figure 8. Our main hypothesis to support this statement is the variation of the mixed layer depth, giving conditions for deeper and stable current during winter and inducing instabilities. In order to verify this hypothesis, an insight of the vertical extent of the surface current and the mixed layer depth variation could be an interesting complementary work.

In addition, we had a closer look at the central Ionian Sea as we observed a non-documented pattern forming a double gyre system associated to the Mid Ionian Jet. We first documented its presence along with temperature profiles and further, made a temporal analysis with mode decomposition with orthogonal functions.

First, we noticed the concomitant acceleration of the MIJ with the appearance of the TGs, both during the second part of the year. Thus, we argue that the TGs are a consequence of the increasing velocities of the MIJ, but not only, as these velocities were already reached without inducing this pattern. We support that the increased velocity of the MIJ along the temperature gradient in the continuity of the Sicily continental slope force the current to flow eastward, being ultimately trapped in gyres, that we decided to call the Twin Gyres. The biogeochemical modifications of the central Ionian Sea are not yet measured but are expected regarding the productivity and the physicochemical properties of this region.

Code availability. https://blue-cloud.d4science.org/group/coastalcurrentsfromobservations

Data availability. https://doi.org/10.5281/zenodo.18860454

Author contributions. AAA, AB and JMB were involved in the development and in the design of the methodology as they developped the DIVAnd method. AAA and AB are the supervisors of the whole work. AAA, AB, JMB and AD were involved for the conceptualization and in shaping the results. AD is the main author, as he conducted the research, performed the experiments and wrote the manuscript. The review and the edition of the manuscript was done by AAA, AB and JMB.

Competing interests. AAA is member of the editorial board of OS.

Acknowledgements. The production of this work has been enabled by D4Science.org www.d4science.org

The production of this work has been enabled by the Coastal Currents from Observations working environment (https://blue-cloud.org/virtual-labs/coastal-currents-observations) via the D4 science gateway operated by D4Science.org www.d4science.org

https://doi.org/10.5194/egusphere-2026-1627
Preprint. Discussion started: 9 April 2026

This manuscript is part of the Blue Cloud 2026 project and is funded by the European Union.

https://doi.org/10.5194/egusphere-2026-1627
Preprint. Discussion started: 9 April 2026

References

Adloff, F., Somot, S., Sevault, F., Jordà, G., Aznar, R., Déqué, M., Herrmann, M., Marcos, M., Dubois, C., Padorno, E., Alvarez-Fanjul, E., and Gomis, D.: Mediterranean Sea response to climate change in an ensemble of twenty first century scenarios, Clim Dyn, 45, 2775–2802, https://doi.org/10.1007/s00382-015-2507-3, 2015.

Alhammoud, B., Béranger, K., Mortier, L., Crépon, M., and Dekeyser, I.: Surface circulation of the Levantine Basin: Comparison of model results with observations, Progress in Oceanography, 66, 299–320, https://doi.org/10.1016/j.pocean.2004.07.015, 2005.

Amitai, Y., Lehahn, Y., Lazar, A., and Heifetz, E.: Surface circulation of the eastern Mediterranean Levantine basin: Insights from analyzing 14 years of satellite altimetry data, J. Geophys. Res., 115, 2010JC006 147, https://doi.org/10.1029/2010JC006147, 2010.

Baaklini, G., Issa, L., Fakhri, M., Brajard, J., Fifani, G., Menna, M., Taupier-Letage, I., Bosse, A., and Mortier, L.: Blending drifters and altimetric data to estimate surface currents: Application in the Levantine Mediterranean and objective validation with different data types, Ocean Modelling, 166, 101 850, https://doi.org/10.1016/j.ocemod.2021.101850, 2021.

Baaklini, G., El Hourany, R., Fakhri, M., Brajard, J., Issa, L., Fifani, G., and Mortier, L.: Surface circulation properties in the eastern Mediterranean emphasized using machine learning methods, Ocean Sci., 18, 1491–1505, https://doi.org/10.5194/os-18-1491-2022, 2022.

Barth, A., Beckers, J.-M., Troupin, C., Alvera-Azcárate, A., and Vandenbulcke, L.: divand-1.0: *n* -dimensional variational data analysis for ocean observations, Geosci. Model Dev., 7, 225–241, https://doi.org/10.5194/gmd-7-225-2014, 2014.

Barth, A., Troupin, C., Reyes, E., Alvera-Azcárate, A., Beckers, J.-M., and Tintoré, J.: Variational interpolation of high-frequency radar surface currents using DIVAnd, Ocean Dynamics, 71, 293–308, https://doi.org/10.1007/s10236-020-01432-x, 2021.

Beckers, J.-M. and Cushman-Roisin, B.: Introduction to Geophysical Fluid Dynamics - Physical and Numerical Aspects, vol. 101 of *International Geophysics*, Elsevier, ISBN 978-0-12-088759-0, https://doi.org/10.1016/C2009-0-00052-X, 2011.

Borzelli, G. L. E., Gačić, M., Cardin, V., and Civitarese, G.: Eastern Mediterranean Transient and reversal of the Ionian Sea circulation, Geophysical Research Letters, 36, https://doi.org/10.1029/2009gl039261, 2009.

Brasseur, P. P. and Haus, J. A.: Application of a 3-D variational inverse model to the analysis of ecohydrodynamic data in the Northern Bering and Southern Chukchi Seas, Journal of Marine Systems, 1, 383–401, https://doi.org/10.1016/0924-7963(91)90006-G, 1991.

Brenner, S.: Structure and evolution of warm core eddies in the eastern Mediterranean Levantine Basin, J. Geophys. Res., 94, 12 593–12 602, https://doi.org/10.1029/JC094iC09p12593, 1989.

Brett, G. J., Pratt, L. J., Rypina, I. I., and Sánchez-Garrido, J. C.: The Western Alboran Gyre: An Analysis of Its Properties and Its Exchange with Surrounding Water, Journal of Physical Oceanography, 50, 3379–3402, https://doi.org/10.1175/JPO-D-20-0028.1, 2020.

Béranger, K., Mortier, L., Gasparini, G.-P., Gervasio, L., Astraldi, M., and Crépon, M.: The dynamics of the Sicily Strait: a comprehensive study from observations and models, Deep Sea Research Part II: Topical Studies in Oceanography, 51, 411–440, https://doi.org/10.1016/j.dsr2.2003.08.004, 2004.

Capodici, F., Cosoli, S., Ciraolo, G., Nasello, C., Maltese, A., Poulain, P.-M., Drago, A., Azzopardi, J., and Gauci, A.: Validation of HF radar sea surface currents in the Malta-Sicily Channel, Remote Sensing of Environment, 225, 65–76, https://doi.org/10.1016/j.rse.2019.02.026, 2019.

Carret, A., Birol, F., Estournel, C., and Zakardjian, B.: Assessing the capability of three different altimetry satellite missions to observe the Northern Current by using a high-resolution model, Ocean Sci., 19, 903–921, https://doi.org/10.5194/os-19-903-2023, 2023.

Ciappa, A.: A study on causes and recurrence of the Mid-Mediterranean Jet from 2003 to 2015 using satellite thermal and altimetry data and CTD casts, Journal of Operational Oceanography, 14, 37–47, https://doi.org/10.1080/1755876X.2019.1632617, 2021.

https://doi.org/10.5194/egusphere-2026-1627
Preprint. Discussion started: 9 April 2026

Civitarese, G., Gačić, M., Batistić, M., Bensi, M., Cardin, V., Dulčić, J., Garić, R., and Menna, M.: The BiOS mechanism: History, theory, implications, Progress in Oceanography, 216, 103 056, https://doi.org/10.1016/j.pocean.2023.103056, 2023.

Copernicus Climate Change Service and Collecte Localisation Satellites: GLOBAL OCEAN GRIDDED L4 SEA SURFACE HEIGHTS AND DERIVED VARIABLES REPROCESSED (COPERNICUS CLIMATE CHANGE SERVICE), https://doi.org/10.48670/MOI-00145, 2021.

Copernicus Marine Service: Global Ocean Gridded L4 Sea Surface Heights And Derived Variables Reprocessed 1993–Ongoing, Dataset, https://doi.org/10.48670/moi-00148, sEALEVEL_GLO_PHY_L4_MY_008_047, 2023.

Corgnati, L., Berta, M., Kokkini, Z., Mantovani, C., Magaldi, M. G., Molcard, A., and Griffa, A.: Assessment of OMA Gap-Filling Performances for Multiple and Single Coastal HF Radar Systems: Validation with Drifter Data in the Ligurian Sea, Remote Sensing, 16, 2458, https://doi.org/10.3390/rs16132458, 2024.

Cotroneo, Y., Aulicino, G., Ruiz, S., Pascual, A., Budillon, G., Fusco, G., and Tintoré, J.: Glider and satellite high resolution monitoring of a mesoscale eddy in the algerian basin: Effects on the mixed layer depth and biochemistry, Journal of Marine Systems, 162, 73–88, https://doi.org/10.1016/j.jmarsys.2015.12.004, 2016.

Delpeche-Ellmann, N., Giudici, A., Rätsep, M., and Soomere, T.: Observations of surface drift and effects induced by wind and surface waves in the Baltic Sea for the period 2011–2018, Journal article, https://doi.org/10.1016/j.ecss.2020.107071, estuarine, Coastal and Shelf Science, Volume 249, Article 107071, 2021.

Demirov, E. and Pinardi, N.: Simulation of the Mediterranean Sea circulation from 1979 to 1993: Part I. The interannual variability, Journal of Marine Systems, 33-34, 23–50, https://doi.org/10.1016/S0924-7963(02)00051-9, 2002.

Dohan, K., Dohan, K., Dohan, K., Dohan, K., Dohan, K., Dohan, K., Dohan, K., Dohan, K., Dohan, K., and Dohan, K.: Measuring the Global Ocean Surface Circulation with Satellite and In Situ Observations, in: Proceedings of OceanObs'09: Sustained Ocean Observations and Information for Society, pp. 237–248, European Space Agency, ISBN 978-3-86987-200-1, https://doi.org/10.5270/OceanObs09.cwp.23, 2010.

Domps, B., Marmain, J., and Guerin, C.-A.: A Reanalysis of the October 2016 "Meteotsunami" in British Columbia With Help of High-Frequency Radars and Autoregressive Modeling, IEEE Geosci. Remote Sensing Lett., 19, 1–5, https://doi.org/10.1109/LGRS.2021.3066849, 2022.

Egorova, V. M., Zyryanov, V. N., and Sokolovskiy, M. A.: The hydrodynamic theory of the Cyprus Eddy, Ocean Dynamics, 72, 1–20, https://doi.org/10.1007/s10236-021-01484-7, 2022.

European Union-Copernicus Marine Service: Global Ocean- in-situ Near real time observations of ocean currents, https://doi.org/10.48670/MOI-00041, 2018.

European Union-Copernicus Marine Service: EUROPEAN SEAS ALONG-TRACK L3 SEA SURFACE HEIGHTS REPROCESSED (1993-ONGOING) TAILORED FOR DATA ASSIMILATION, https://doi.org/10.48670/MOI-00139, 2021.

Frissell, N. A., Baker, J. B. H., Ruohoniemi, J. M., Greenwald, R. A., Gerrard, A. J., Miller, E. S., and West, M. L.: Sources and characteristics of medium-scale traveling ionospheric disturbances observed by high-frequency radars in the North American sector, JGR Space Physics, 121, 3722–3739, https://doi.org/10.1002/2015JA022168, 2016.

Iacono, R., Napolitano, E., Marullo, S., Artale, V., and Vetrano, A.: Seasonal Variability of the Tyrrhenian Sea Surface Geostrophic Circulation as Assessed by Altimeter Data, Journal of Physical Oceanography, 43, 1710–1732, https://doi.org/10.1175/JPO-D-12-0112.1, 2013.

https://doi.org/10.5194/egusphere-2026-1627
Preprint. Discussion started: 9 April 2026

Iacono, R., Napolitano, E., Palma, M., and Sannino, G.: The Tyrrhenian Sea Circulation: A Review of Recent Work, Sustainability, 13, 6371, https://doi.org/10.3390/su13116371, 2021.

Jebri, F., Birol, F., Zakardjian, B., Bouffard, J., and Sammari, C.: Exploiting coastal altimetry to improve the surface circulation scheme over the central Mediterranean Sea, JGR Oceans, 121, 4888–4909, https://doi.org/10.1002/2016JC011961, 2016.

Jebri, F., Zakardjian, B., Birol, F., Bouffard, J., Jullion, L., and Sammari, C.: Interannual Variations of Surface Currents and Transports in the Sicily Channel Derived From Coastal Altimetry, JGR Oceans, 122, 8330–8353, https://doi.org/10.1002/2017JC012836, 2017.

Jouini, M., Béranger, K., Arsouze, T., Beuvier, J., Thiria, S., Crépon, M., and Taupier-Letage, I.: The Sicily Channel surface circulation revisited using a neural clustering analysis of a high-resolution simulation, JGR Oceans, 121, 4545–4567, https://doi.org/10.1002/2015JC011472, 2016.

Juza, M., Heslop, E., Zarokanellos, N. D., and Tintoré, J.: Multi-scale ocean variability in the Ibiza Channel over 14-year repeated glider missions, Front. Mar. Sci., 12, 1604 087, https://doi.org/10.3389/fmars.2025.1604087, 2025.

Kalimeris, A. and Kassis, D.: Sea surface circulation variability in the Ionian-Adriatic Seas, Progress in Oceanography, 189, 102 454, https://doi.org/10.1016/j.pocean.2020.102454, 2020.

Le Traon, P.-Y., Dibarboure, G., Lellouche, J.-M., Pujol, M.-I., Benkiran, M., Drevillon, M., Drillet, Y., Faugère, Y., and Remy, E.: Satellite altimetry and operational oceanography: from Jason-1 to SWOT, Ocean Science, 21, 1329–1347, https://doi.org/10.5194/os-21-1329-2025, 2025.

Lee, S. and Song, H.: Quantifying the inflation factors of observation error variance for COMS and MTSAT A tmospheric Motion Vectors considering spatial observation error correlation, Quart J Royal Meteoro Soc, 143, 2625–2635, https://doi.org/10.1002/qj.3113, 2017.

Liu, F., Zhou, H., Huang, W., and Wen, B.: Submesoscale Eddies Observation Using High-Frequency Radars: A Case Study in the Northern South China Sea, IEEE J. Oceanic Eng., 46, 624–633, https://doi.org/10.1109/JOE.2020.2986175, 2021.

Liu, F., Mikolajewicz, U., and Six, K. D.: Drivers of the decadal variability of the North Ionian Gyre upper layer circulation during 1910–2010: a regional modelling study, Clim Dyn, 58, 2065–2077, https://doi.org/10.1007/s00382-021-05714-y, 2022.

Lumpkin, R. and Johnson, G. C.: Global ocean surface velocities from drifters: Mean, variance, El Niño–Southern Oscillation response, and seasonal cycle, JGR Oceans, 118, 2992–3006, https://doi.org/10.1002/jgrc.20210, 2013.

Lumpkin, R. and Pazos, M.: Measuring surface currents with Surface Velocity Program drifters: the instrument, its data, and some recent results, in: Lagrangian Analysis and Prediction of Coastal and Ocean Dynamics, edited by Griffa, A., Kirwan, Jr., A. D., Mariano, A. J., Özgökmen, T., and Rossby, H. T., pp. 39–67, Cambridge University Press, 1 edn., ISBN 978-0-521-87018-4 978-0-511-53590-1, https://doi.org/10.1017/CBO9780511535901.003, 2007.

Malanotte-Rizzoli, P., Artale, V., Borzelli-Eusebi, G. L., Brenner, S., Crise, A., Gacic, M., Kress, N., Marullo, S., Ribera d'Alcalà, M., Sofianos, S., Tanhua, T., Theocharis, A., Alvarez, M., Ashkenazy, Y., Bergamasco, A., Cardin, V., Carniel, S., Civitarese, G., D'Ortenzio, F., Font, J., Garcia-Ladona, E., Garcia-Lafuente, J. M., Gogou, A., Gregoire, M., Hainbucher, D., Kontoyannis, H., Kovacevic, V., Kraskapoulou, E., Kroskos, G., Incarbona, A., Mazzocchi, M. G., Orlic, M., Ozsoy, E., Pascual, A., Poulain, P.-M., Roether, W., Rubino, A., Schroeder, K., Siokou-Frangou, J., Souvermezoglou, E., Sprovieri, M., Tintoré, J., and Triantafyllou, G.: Physical forcing and physical/biochemical variability of the Mediterranean Sea: a review of unresolved issues and directions for future research, Ocean Sci., 10, 281–322, https://doi.org/10.5194/os-10-281-2014, 2014.

https://doi.org/10.5194/egusphere-2026-1627
Preprint. Discussion started: 9 April 2026

Mallil, K., Testor, P., Bosse, A., Margirier, F., Houpert, L., Le Goff, H., Mortier, L., and Louanchi, F.: The Levantine Intermediate Water in the western Mediterranean and its interactions with the Algerian Gyres: insights from 60 years of observation, Ocean Sci., 18, 937–952, https://doi.org/10.5194/os-18-937-2022, 2022.

Martínez, J., García-Ladona, E., Ballabrera-Poy, J., Isern-Fontanet, J., González-Motos, S., Allegue, J. M., and González-Haro, C.: Atlas of surface currents in the Mediterranean and Canary–Iberian–Biscay waters, Journal of Operational Oceanography, 17, 40–62, https://doi.org/10.1080/1755876x.2022.2102357, 2024.

Meli, M.: The potential recording of North Ionian Gyre's reversals as a decadal signal in sea level during the instrumental period, Sci Rep, 14, 4907, https://doi.org/10.1038/s41598-024-55579-4, 2024.

Menna, M., Poulain, P.-M., Ciani, D., Doglioli, A., Notarstefano, G., Gerin, R., Rio, M.-H., Santoleri, R., Gauci, A., and Drago, A.: New Insights of the Sicily Channel and Southern Tyrrhenian Sea Variability, Water, 11, 1355, https://doi.org/10.3390/w11071355, 2019a.

Menna, M., Suarez, N. R., Civitarese, G., Gačić, M., Rubino, A., and Poulain, P.-M.: Decadal variations of circulation in the Central Mediterranean and its interactions with mesoscale gyres, Deep Sea Research Part II: Topical Studies in Oceanography, 164, 14–24, https://doi.org/10.1016/j.dsr2.2019.02.004, 2019b.

Mkhinini, N., Coimbra, A. L. S., Stegner, A., Arsouze, T., Taupier-Letage, I., and Béranger, K.: Long-lived mesoscale eddies in the eastern Mediterranean Sea: Analysis of 20 years of AVISO geostrophic velocities, JGR Oceans, 119, 8603–8626, https://doi.org/10.1002/2014JC010176, 2014.

Napolitano, E., Carillo, A., Struglia, M., Iacono, R., Palma, M., Borzelli, G. E., and Sannino, G.: The role of the Atlantic-Ionian stream in the long-term variability of the surface circulation in the Northern Ionian Sea: Results from a hindcast simulation, Progress in Oceanography, 234, 103 472, https://doi.org/10.1016/j.pocean.2025.103472, 2025.

Pessini, F., Olita, A., Cotroneo, Y., and Perilli, A.: Mesoscale eddies in the Algerian Basin: do they differ as a function of their formation site?, Ocean Sci., 14, 669–688, https://doi.org/10.5194/os-14-669-2018, 2018.

Pinardi, N., Zavatarelli, M., Adani, M., Coppini, G., Fratianni, C., Oddo, P., Simoncelli, S., Tonani, M., Lyubartsev, V., Dobricic, S., and Bonaduce, A.: Mediterranean Sea large-scale low-frequency ocean variability and water mass formation rates from 1987 to 2007: A retrospective analysis, Progress in Oceanography, 132, 318–332, https://doi.org/10.1016/j.pocean.2013.11.003, 2015.

Poje, A. C., Özgökmen, T. M., Lipphardt, B. L., Haus, B. K., Ryan, E. H., Haza, A. C., Jacobs, G. A., Reniers, A. J. H. M., Olascoaga, M. J., Novelli, G., Griffa, A., Beron-Vera, F. J., Chen, S. S., Coelho, E., Hogan, P. J., Kirwan, A. D., Huntley, H. S., and Mariano, A. J.: Submesoscale dispersion in the vicinity of the *Deepwater Horizon* spill, Proc. Natl. Acad. Sci. U.S.A., 111, 12 693–12 698, https://doi.org/10.1073/pnas.1402452111, 2014.

Poulain, P.-M.: Aspects of the Surface Circulation in the Liguro-Provençal Basin and Gulf of Lion As Observed By Satellite-Tracked Drifters (2007-2009), https://doi.org/10.4430/bgta0052, 2012.

Poulain, P.-M., Bussani, A., Gerin, R., Jungwirth, R., Mauri, E., Menna, M., and Notarstefano, G.: Mediterranean Surface Currents Measured with Drifters: From Basin to Subinertial Scales, oceanog, 26, 38–47, https://doi.org/10.5670/oceanog.2013.03, 2013.

Renault, L., Oguz, T., Pascual, A., Vizoso, G., and Tintore, J.: Surface circulation in the Alborán Sea (western Mediterranean) inferred from remotely sensed data, J. Geophys. Res., 117, 2011JC007 659, https://doi.org/10.1029/2011JC007659, 2012.

Sammari, C., Millot, C., Taupier-Letage, I., Stefani, A., and Brahim, M.: Hydrological characteristics in the Tunisia–Sardinia–Sicily area during spring 1995, Deep Sea Research Part I: Oceanographic Research Papers, 46, 1671–1703, https://doi.org/10.1016/S0967-0637(99)00026-6, 1999.

https://doi.org/10.5194/egusphere-2026-1627
Preprint. Discussion started: 9 April 2026

Soto-Navarro, J., Criado-Aldeanueva, F., García-Lafuente, J., and Sánchez-Román, A.: Estimation of the Atlantic inflow through the Strait of Gibraltar from climatological and in situ data, J. Geophys. Res., 115, 2010JC006 302, https://doi.org/10.1029/2010JC006302, 2010.

Soto-Navarro, J., Lorente, P., Álvarez Fanjul, E., Carlos Sánchez-Garrido, J., and García-Lafuente, J.: Surface circulation at the S trait of G ibraltar: A combined HF radar and high resolution model study, JGR Oceans, 121, 2016–2034, https://doi.org/10.1002/2015JC011354, 2016.

Testor, P., Send, U., Gascard, J., Millot, C., Taupier-Letage, I., and Béranger, K.: The mean circulation of the southwestern Mediterranean Sea: Algerian Gyres, J. Geophys. Res., 110, 2004JC002 861, https://doi.org/10.1029/2004JC002861, 2005.

Troupin, C., Machín, F., Ouberdous, M., Sirjacobs, D., Barth, A., and Beckers, J.: High-resolution climatology of the northeast Atlantic using Data-Interpolating Variational Analysis (Diva), J. Geophys. Res., 115, 2009JC005 512, https://doi.org/10.1029/2009JC005512, 2010.

Troupin, C., Beltran, J. P., Frontera, B., Gómara, S., Lora, S., March, D., Sebastian, K., and Tintoré, J.: Oceanographic data management at the Balearic Islands Coastal Ocean Observing and Forecasting System (SOCIB), 2015.

Vargas-Yáñez, M., Sánchez-Leal, R. F., Alvera-Azcárate, A., Troupin, C., Moya, F., Ballesteros, E., Serra, M., Balbín, R., Moltó, V., and García-Martínez, M. C.: Opportunity observation of an Algerian Eddy to the south of Cape Palos (southwestern Mediterranean Sea), Sci. mar., 87, e070, https://doi.org/10.3989/scimar.05333.070, 2023.

Vargas-Yáñez, M., Ouradou, M., Moya, F., Ballesteros, E., Alonso, C., Serra, M., Piñeiro, S., Moltó, V., Santiago, R., Balbín, R., Sánchez-Aguado, S., García-Martínez, M. C., Jordà, G., and Hernández-Guerra, A.: A time series of water mass transports through the Balearic Channels using an ocean circulation inverse method: 1996–2022, Progress in Oceanography, 237, 103 525, https://doi.org/10.1016/j.pocean.2025.103525, 2025.

Verma, V., Barkan, R., Solodoch, A., Gildor, H., and Toledo, Y.: The Eastern Mediterranean Boundary Current: Seasonality, Stability, and Spiral Formation, Journal of Physical Oceanography, 54, 1971–1989, https://doi.org/10.1175/JPO-D-23-0207.1, 2024.

Wilkinson, R., Mleczko, M., Brewin, R., Gaston, K., Mueller, M., Shutler, J., Yan, X., and Anderson, K.: Environmental impacts of earth observation data in the constellation and cloud computing era, Science of The Total Environment, 909, 168 584, https://doi.org/10.1016/j.scitotenv.2023.168584, 2024.

Zodiatis, G., Brenner, S., Gertman, I., Ozer, T., Simoncelli, S., Ioannou, M., and Savva, S.: Twenty years of in-situ monitoring in the south-eastern Mediterranean Levantine basin: Basic elements of the thermohaline structure and of the mesoscale circulation during 1995-2015, Front. Mar. Sci., 9, https://doi.org/10.3389/fmars.2022.1074504, 2023.